The Dynamics of Ultrafast Excited State Proton Transfer in Anionic Micelles†

Letícia Giestas,‡ Chang Yihwa,§ João C. Lima,‡,|| Carolina Vautier-Giongo,§ António Lopes,‡ Antonio L. Maçanita,‡,⊥ and Frank H. Quina*,‡

Instituto de Tecnologia Química e Biológica, ITQB/UNL, Oeiras Portugal, Chemical Systems Engineering Group, Instituto de Química, Universidade de São Paulo, CP 26077, São Paulo 05513-970, Brazil, and Departamento de Química, IST/UTL, Lisbon, Portugal

Received: July 23, 2002

Fast excited state proton transfer reactions at the surface of anionic sodium dodecyl sulfate (SDS) micelles have been investigated using the photoacid 4-methyl-7-hydroxyflavylium (HMF) chloride as probe. The acid−base kinetics of excited HMF are straightforward in water, with biexponential fluorescence decays reflecting ultrafast deprotonation of the excited acid $(AH^+)^*$ ($k_d = 1.5 \times 10^{11}$ s^{-1} or ca. 6 ps) and diffusion-controlled protonation of the excited base A* ($k_p = 2.3 \times 10^{10}$ L mol^{-1} s^{-1} at 20 °C). In aqueous micellar SDS solutions, the kinetics are much more complex; triple exponential fluorescence decays are observed at all pH values and temperatures examined. The longest decay time ($\tau_1 = 760$ ps at 22 °C), observed only for $(AH^+)^*$ and uncoupled from the acid−base equilibrium, is assigned to excitation of HMF in orientations incapable of prompt transfer of the proton to water, i.e., that must rotate to expose the acidic OH group to water ($k_{rot} = 1.2 \times 10^9$ s^{-1} or ca. 800 ps at 22 °C). The other two decay times, τ_3 and τ_2, are due to emission from the species involved in the acid−base reaction at the micelle surface. Deprotonation of $(AH^+)^*$ is slightly slower in SDS micelles ($k_d = 3.4 \times 10^{10}$ s^{-1} or ca. 20 ps) than in water. Two processes are operative in the back protonation of A*: (i) pH-independent unimolecular reprotonation in the initially formed geminate compartmentalized pair ($A^*\cdots H_3O^+$) ($k_r = 8.8 \times 10^9$ s^{-1}) and (ii) pH-dependent bimolecular protonation of A* via entry of an aqueous phase proton into the micelle ($k_p = 1.6 \times 10^{11}$ M^{-1} s^{-1}). Dissociation of the geminate pair ($k_{diss} = 1.6 \times 10^9$ s^{-1}) forms A* at the micellar surface. The present study thus provides a rather detailed kinetic picture of the initial steps involved in an ultrafast excited state proton transfer process at the surface of a typical anionic micelle.

Introduction

Proton transfer reactions have been so extensively studied that very few features of this type of reaction remain to be elucidated.[1,2] This is true even though kinetic data are absent for many of these reactions in water, particularly for those with deprotonation rates that fall into the experimentally difficult subnanosecond and submicrosecond time ranges.[3]

Charged interfaces, such as the surface of an ionic detergent micelle, can dramatically modify both the kinetics and the energetics of such reactions with respect to their normal characteristics in aqueous solution.[4] The most obvious perturbation is the introduction of heterogeneities in the distribution of ionic reactants in the solution due to electrostatic interactions with the charged interface. Thus, the concentration of protons at a negatively charged micellar surface is higher than that in the bulk aqueous phase and the reverse is true for positively charged surfaces.[4,5] Although many studies of micellar effects on proton transfer equilibria have been reported, the effects of charged interfaces on the rate constants and activation energies of proton transfer have been less thoroughly investigated. In addition to modifying the effective local concentration of protons, the interface can also exert an even greater intrinsic effect on the rates due to differential stabilization or destabilization of the species involved in the proton transfer equilibria. For instance, the rate constant for deprotonation of the 4-methyl-7-hydroxyflavylium cation (HMF) decreases by 2 orders of magnitude upon going from water (10^6 s^{-1} range) to anionic sodium dodecyl sulfate (SDS) micelles (10^4 s^{-1} range). This decrease in the rate constant reflects the preferential stabilization of the flavylium cation by the anionic micelle relative to the neutral anhydrobase form.[6] Analogous effects of SDS micelles on deprotonation rate constants have been observed for the naturally occurring anthocyanin oenin.[7]

Given the magnitude of these effects on the rates of ground state proton transfer processes, we were interested in examining the effect of SDS micelles on the much faster excited state proton transfer reactions of HMF. Indeed, the excited singlet state of HMF has one of the highest (if not the highest) known rate constants for deprotonation to water ($k_d = 1.5 \times 10^{11}$ s^{-1}),[8] making it a particularly appropriate molecule for probing ultrafast proton transfer reactions in organized media. In addition, in aqueous solution in the absence of micelles, the acid−base kinetics of excited HMF are straightforward, and the fluorescence of both the excited acid $(AH^+)^*$ and the base (A*) forms exhibits the expected biexponential decay.[8]

The results of the present study point to significant differences between the excited state proton transfer process of HMF in water and at the surface of anionic SDS micelles. In particular,

† Part of the special issue "George S. Hammond & Michael Kasha Festschrift".

* To whom correspondence should be addressed. E-mail: quina@usp.br.
‡ Instituto de Tecnologia Química e Biológica.
§ Universidade de São Paulo.
|| Present address: REQUIMTE/CQFB, Departamento de Química, FCT/UNL, Portugal.
⊥ IST/UTL.

10.1021/jp0265900 CCC: $25.00 © 2003 American Chemical Society
Published on Web 01/07/2003

kinetic analysis shows that the proton transfer at the micelle surface proceeds via the intermediacy of a finite-lived micelle-compartmentalized geminate pair ($A^*\cdots H_3O^+$), which either recombines to regenerate $(AH^+)^*$ or dissociates to A*.

Experimental Section

HMF was synthesized and purified as previously described.[8] SDS and sodium phosphate and chloride, pa, from Sigma were used as received. Samples were prepared in buffered (24 mM phosphate) aqueous solutions of SDS (100 mM), employing bidistilled, deionized (Elgastat UHQ PS) water. The concentration of HMF was typically ca. 10^{-5} M.

The pH values were measured at 20 °C employing a Crison 2002 micropH Meter with a Mettler Toledo HA405-60-88TE-S7 combination electrode. UV−vis absorption spectra were recorded on a Beckman DU-70 spectrophotometer, and corrected fluorescence spectra were recorded on a SPEX Fluorolog 2 fluorimeter.

Fluorescence decays were measured using the time-correlated single photon counting technique employing an excitation source consisting of a mode-locked Ti−Sapphire laser (Spectra-Physics Tsunami) pumped by a Millenia X (Spectra-Physics) laser. The pulse repetition rate at the output of the Tsunami (82 MHz) was reduced to 4 MHz with an optoacoustic modulator (Spectra-Physics Pulse Selector model 3980). The light frequency of the Tsunami output (840 nm) was doubled using a second harmonic generator LBO crystal. Light pulses were monitored with a fast photodiode, filtered in a constant fraction discriminator (Canberra 2126), and used as stop signals in a time-to-amplitude converter (Canberra 2145 TAC). The horizontally polarized excitation beam (427 nm) was first depolarized (Oriel depolarizer ref 28110), and then vertically polarized, and passed through a continuous neutral density filter. Fluorescence emission was collected at 90° geometry, passed through a polarizer at approximately 54.7° (Spindler & Hoyer Glan laser prism polarizer) and a monochromator (Jobin-Yvon H20 Vis), and detected with a microchannel plate photomultiplier (Hamamatsu R3809u-50 MCPT). The MCPT signal was filtered with a second Canberra 2126 and used as the start signal for the TAC. Automatic alternate measurements (10^3 counts at the maximum per cycle) of the excitation pulse profile and sample emissions were made until a typical value of 5×10^3 total counts had been accumulated at the maximum. Fluorescence decays were deconvoluted from the excitation pulse using G. Striker's Sand program, which allows individual and global analysis of the decays with individual shift optimization.[9]

Results

Figure 1 shows absorption and fluorescence spectra of HMF in 0.10 M micellar SDS solutions at various values of the pH of the intermicellar aqueous phase. The absorption spectra (Figure 1a) exhibit the absorption bands of the acid form (AH^+) of HMF at $\lambda_{max} = 427$ nm and the conjugate base form (A) at $\lambda_{max} = 475$ nm. The substantial red shift with respect to aqueous solution ($\lambda_{max} = 416.5$ nm and $\lambda_{max} = 464$ nm, respectively) is unaffected by further addition of SDS, consistent with essentially complete incorporation of both forms into the micellar pseudophase under our conditions. The value of the apparent pK_a in 0.10 M SDS (p$K_a = 6.70$)[6] is substantially higher than that in water (p$K_a = 4.45$).[8]

The fluorescence spectra ($\lambda_{exc} = 420$ nm) exhibit the emission of the excited acid $(AH^+)^*$ and base A* forms at 490 and 618 nm, respectively. The emission of $(AH^+)^*$ is much more intense in micellar SDS than in water.[8] Excitation spectra monitored at either 490 or 618 nm are identical to the absorption spectrum of AH^+ alone at all pH values where the flavylium cation is the only species present in the ground state. This implies that A* is formed via adiabatic deprotonation of AH^+ in the excited state, as found in water.[8]

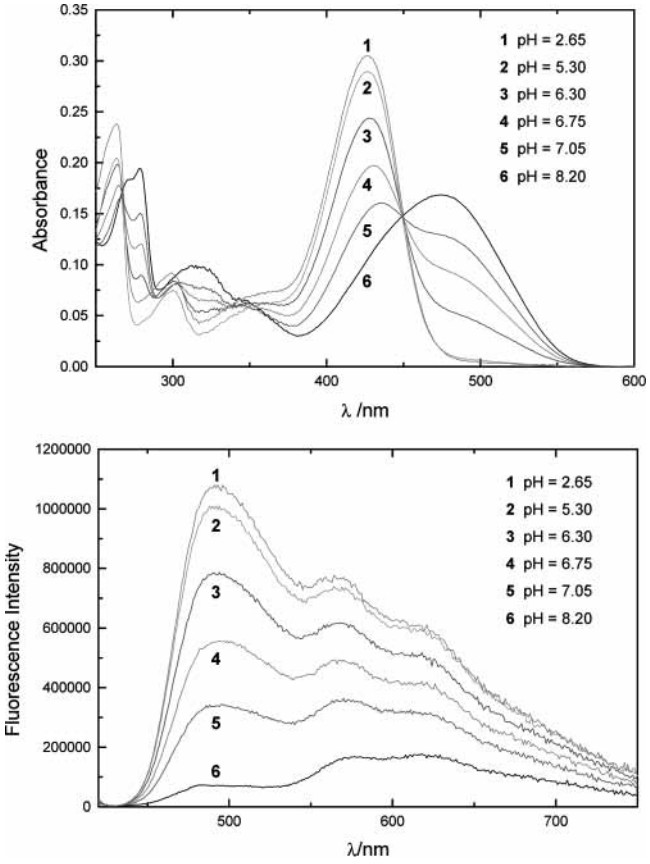

Figure 1. (a) Absorption spectra of HMF ($\sim 1 \times 10^{-5}$ M) in 0.10 M aqueous SDS solutions at 20 °C as a function of the pH of the intermicellar aqueous phase: (1) pH = 2.65; (2) pH = 5.30; (3) pH = 6.30; (4) pH = 6.75; (5) pH = 7.05; and (6) pH = 8.20. At pH = 2.65, the absorption spectrum is that of the cationic form, AH^+ ($\lambda_{max} = 427$ nm); at pH = 8.2, it is practically that of the base form, A ($\lambda_{max} = 475$ nm). (b) Fluorescence spectra of the same solutions at 20 °C, with excitation at 420 nm.

Fluorescence decays of HMF, measured at 480 nm (emission of $(AH^+)^*$) and 630 nm (A* emission) are triple exponentials in micellar SDS at all pH values examined, as opposed to water where they could be fit with the sum of only two exponentials.[8] Global analyses of an example of such decays are shown in Figure 2, and the results are summarized in Table 1.

The two shorter decay times ($\tau_3 \approx 20$ ps and $\tau_2 \approx 220$ ps) are similar in magnitude, to the two times found in water (5.5 and 130 ps, at 20 °C), and τ_3 appears as a growth in the decay of A* at 600 nm. In water, these two lifetimes are present at all wavelengths and are related to the decays of the kinetically coupled $(AH^+)^*$ and A* species.[8]

The third decay time ($\tau_1 \approx 760$ ps), present in micellar SDS but absent in water, is much longer than the other two lifetimes and is observed only at wavelengths where $(AH^+)^*$ emits. Thus, at wavelengths longer than 600 nm, this longest lifetime component (τ_1) vanishes and the decays simplify to double exponentials. On the other hand, at 480 nm, this component accounts for most of the observed fluorescence, i.e., it is this longest lived species that is largely responsible for the much more intense fluorescence of $(AH^+)^*$ in SDS micelles with respect to water.

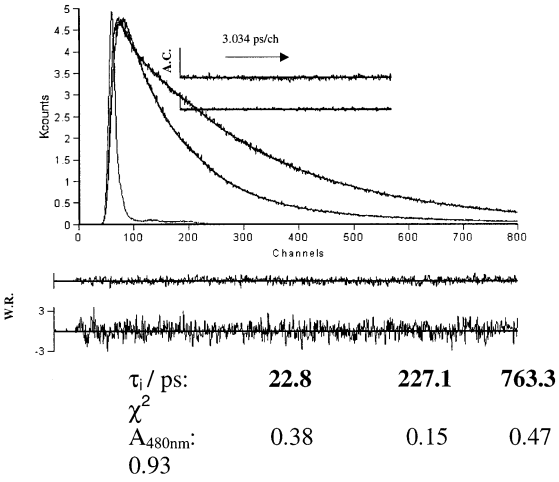

Figure 2. Fluorescence decays of HMF, measured at 480 (AH^+ emission) and 600 nm (A emission) in 0.10 M SDS at pH = 2.31. Global analysis of the decays, autocorrelation functions (AC), and weighted residuals (WR) are also shown.

TABLE 1: Lifetimes (τ_i) and Preexponential Coefficients (A_i) Derived from Fits of HMF Fluorescence Decays at 480 nm in 0.10 M SDS at 22 °C

pH	τ_3 (ps)	τ_2 (ps)	τ_1 (ps)	A_3	A_2	A_1	$R = A_3/A_2$
1.3	18.2	222	762	0.37	0.17	0.46	2.18
1.4	17.9	222	763	0.35	0.16	0.49	2.20
1.5	20.0	221	764	0.37	0.17	0.46	2.24
1.7	23.9	218	752	0.42	0.17	0.41	2.46
2.0	23.3	217	737	0.44	0.16	0.40	2.75
2.31	22.8	227	763	0.43	0.13	0.44	3.31
3.51	24.3	227	746	0.43	0.12	0.45	3.48
4.55	21.2	226	764	0.40	0.11	0.48	3.59
5.79	23.7	222	760	0.37	0.12	0.51	3.21
6.90	18.2	218	772	0.46	0.12	0.42	3.96

Figure 3 shows plots of the decay times (τ_i) and preexponential coefficients (A_i) of $(AH^+)^*$ in micellar SDS from global analysis, as a function of the pH of the intermicellar aqueous phase. Surprisingly, all of the data (τ_i and A_i) are practically independent of the aqueous phase pH. Particularly noteworthy is the fact that the amplitude ratio A_3/A_2, which reflects the pH-dependent back protonation, does not exhibit appreciable variation. This behavior is in marked contrast to water, where this ratio increases strongly with increasing pH,[8] reflecting the fact that at sufficiently high pH, back protonation of the excited state becomes kinetically unimportant ($k_p[H^+] \ll k_A$ and A_2 tends to 0).

In Figure 4, the effect of temperature on the decay times (τ_i) and preexponential coefficients (A_i) of $(AH^+)^*$ at pH = 5.7 in micellar SDS is shown. All decay times decrease with increasing temperature, but again, the amplitude ratio A_3/A_2 does not vary appreciably. The lifetime of the base form, obtained from the single exponential decay of A* at 630 nm measured at pH = 8.8, where only A is present in the ground state, is indistinguishable from τ_2, as indicated in Figure 4a.

Discussion

HMF exhibits the simplest possible ground state chemistry of flavylium salts in aqueous solution. In acidic solutions (pH < 7), only the flavylium cation, AH^+, and the quinonoidal base, A, are detected ($pK_a = 4.45$) and the proton transfer kinetics are characterized by first-order deprotonation ($k_d = 1.4 \times 10^6$ s^{-1}) and diffusion-controlled protonation ($k_p = 3.6 \times 10^{10}$ L mol^{-1} s^{-1}).[3] In the ground state, micellar SDS does not qualitatively change this picture (only two species and simple

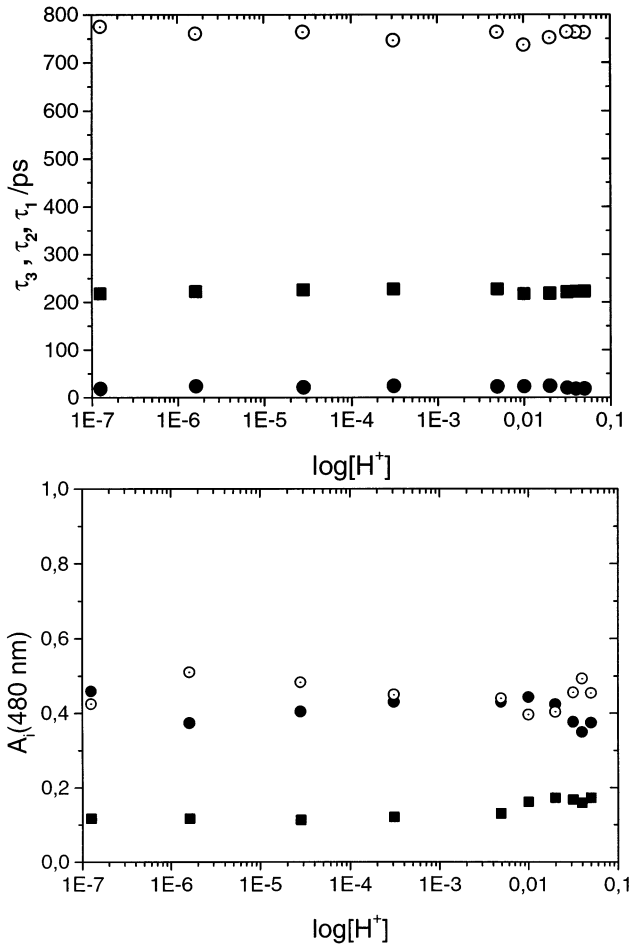

Figure 3. pH dependence of the lifetimes and preexponential coefficients at 480 nm derived from the fits of the fluorescence decays of HMF in 0.10 M SDS at 20 °C: (●) τ_3 and A_3, (■) τ_2 and A_2, and (○) τ_1 and A_1.

kinetics are still observed), although the deprotonation and protonation rate constants are substantially modified ($k_d = 3.6 \times 10^4$ s^{-1} and $k_p = 1.8 \times 10^{11}$ L mol^{-1} s^{-1}), resulting in a much higher apparent pK_a of 6.7.[6]

In aqueous solution, the excited state kinetics of HMF are also relatively simple, i.e., the fluorescence spectra show exclusively the emissions of excited AH^+ and A and both emissions decay as double exponentials. The excited state rate constants are $k_d = 1.5 \times 10^{11}$ s^{-1} and $k_p = 2.3 \times 10^{10}$ L mol^{-1} s^{-1}.[8] However, as shown in the Results section, in the presence of SDS micelles, the excited state proton transfer kinetics become much more complex. The first evident difference with respect to water is the occurrence of a third, much longer decay time (τ_1) in the emission of $(AH^+)^*$. Visual inspection of the decays (Figure 2) shows that as a consequence of the presence of this long lifetime, the decays of $(AH^+)^*$ and A* eventually cross each other, i.e., the fluorescence of $(AH^+)^*$ persists much longer than that of A*.

Whatever τ_1 represents, it does not produce A* and is consequently kinetically uncoupled from the acid−base equilibrium. On the other hand, excitation spectra and dilution below the critical micelle concentration (where the long lifetime component disappears) prove that τ_1 is due to emission from $(AH^+)^*$ associated with the micellar phase. This strongly suggests that the long lifetime corresponds to emission from a subpopulation of micellar $(AH^+)^*$ that for some reason, cannot efficiently deprotonate to water during its intrinsic lifetime (130 ps in water[8] but as long as 5 ns in organic solvents such as

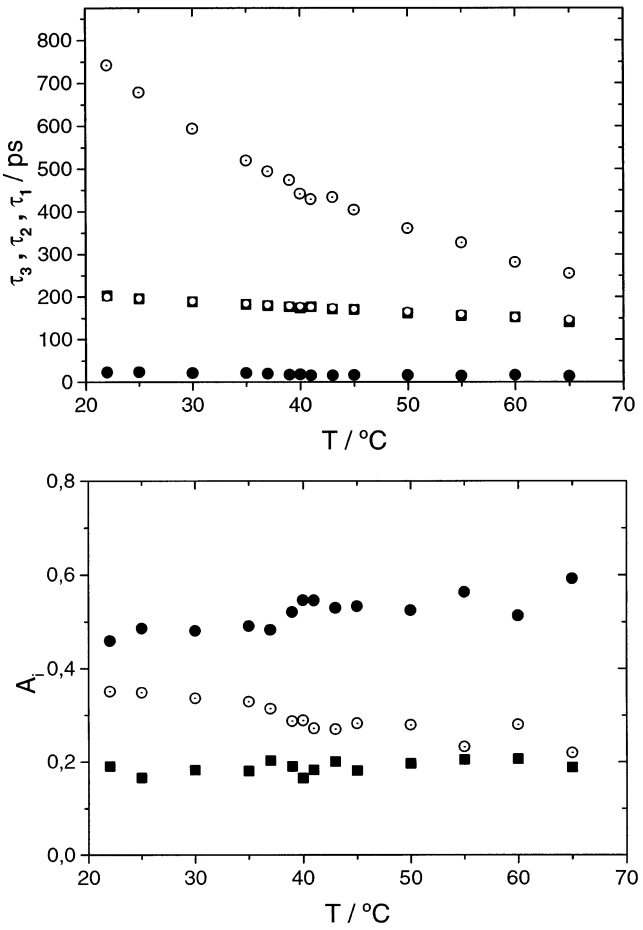

Figure 4. Temperature dependence of the lifetimes and preexponential coefficients at 480 nm obtained from the fits of the fluorescence decays of HMF in 0.10 M SDS at pH 5.7: (●) τ_3 and A_3, (■) τ_2 and A_2, (○) τ_1 and A_1, and (○) fluorescence lifetimes of the base A at pH = 8.8.

acetonitrile). A plausible explanation is that a certain fraction of the micelle-incorporated AH^+ molecules is excited in an orientation in which there is no neighboring water molecule to which the OH group can transfer its proton immediately after excitation. Evidently, the most likely orientation would be one in which the OH group of HMF points into the interior of the micelle. Molecules oriented in this manner would have to undergo a molecular rotation in order to react, which for a large cationic organic molecule in an anionic SDS micelle, may take upward of several hundred picoseconds.[10]

Assuming, then, that the rate-limiting step for excited state decay is rotation rather than proton transfer, the reciprocal of τ_1 should be determined by the sum of the inherent decay rate of $(AH^+)^*$ in the absence of deprotonation, k_{AH^+}, and the rotational rate constant of $(AH^+)^*$ in the micelle, k_{rot} (eq 1):

$$\lambda_1 = 1/\tau_1 = k_{AH^+} + k_{rot} \qquad (1)$$

Values of k_{AH^+} were estimated from the single exponential lifetime of the analogous parent compound 7-methoxy-4-methylflavylium chloride (which cannot deprotonate) in SDS micelles under the same conditions (k_{AH^+} varies from 1.77×10^8 s^{-1} at 22 °C to 2.05×10^8 s^{-1} at 65 °C) and these were subtracted from λ_1 to yield k_{rot} values as a function of temperature. At 20 °C, the value of k_{rot} is 1.2×10^9 s^{-1}, corresponding to a rotational reorientation time of ca. 800 ps, in the range of reported values of probes in SDS micelles.[10] Figure 5 shows the Arrhenius plot for k_{rot}. The value of the apparent activation energy obtained from this plot, $E_{rot} = 22$ kJ mol^{-1}, is consistent with the magnitude of viscosity values found for SDS (14−19 cP range[11]). Thus, on a plot of ln η vs E_η for alkanes, $E_\eta = 26$ kJ mol^{-1} corresponds to a mean value of $\eta = 17$ cP.

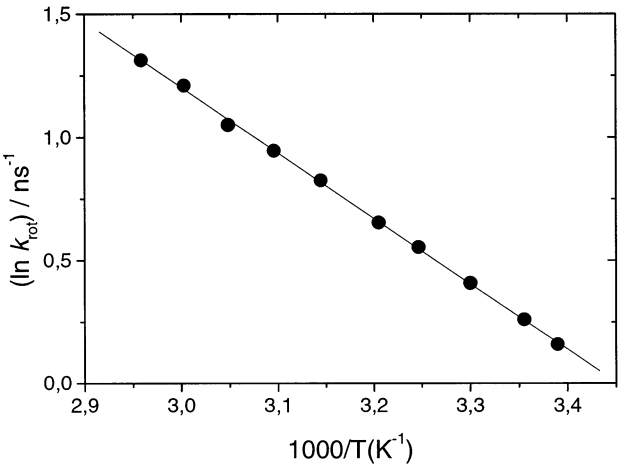

Figure 5. Arrhenius plot of the rotational rate constant, k_{rot}, of AH^+ in 0.10 M aqueous SDS.

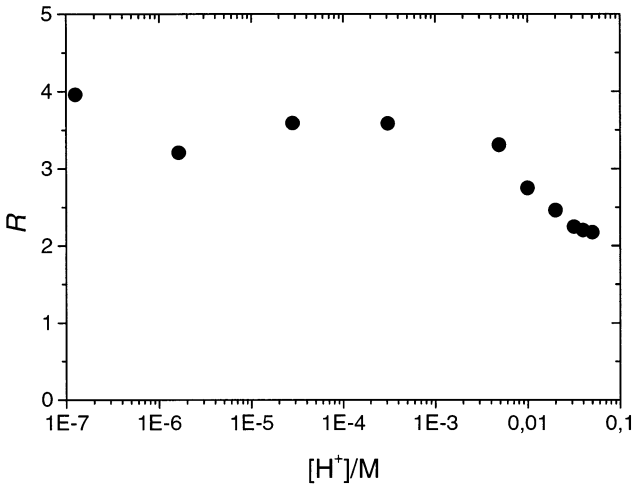

Figure 6. Plot of the ratio of the preexponential coefficients in the decays of $(AH^+)^*$ at 480 nm, $R = A_3/A_2$, as a function of $[H^+]$.

Analysis of the Coupled Acid−Base Reaction. The remaining fraction of micellar AH^+ that is appropriately oriented for prompt proton transfer at the moment of excitation, i.e., with the OH group in contact with water at the micelle surface, participates in the coupled acid−base reaction, giving rise to the emissions with the two shorter decay times, τ_3 and τ_2. Here, however, there is another major difference with respect to the kinetics in water. In water at pH = 3, the ratio of the preexponential coefficients for the decay of $(AH^+)^*$ at 480 nm, $R = A_3/A_2$, is ca. 300. In the presence of micellar SDS, the magnitude of R is substantially smaller and displays a quite unusual variation with the pH, as depicted in Figure 6. At more acidic pH values ($[H^+] > 10^{-3}$ M), the rate of protonation of A* back to $(AH^+)^*$ increases with increasing $[H^+]$. Consequently, the contribution of the longer component to the decay of AH^+ increases (A_2 increases) and R decreases as expected. In contrast, for $[H^+] < 10^{-3}$ M, R levels off at a value of 3.6 ± 0.4 instead of continuously increasing with increasing pH. This leveling off of R at pH > 3 implies that excited AH^+ is being efficiently formed at the expense of A* via a mechanism that is pH-independent but capable of competing with the very fast, subnanosecond decay of A* to the ground state ($k_A = 5 \times 10^9$ s^{-1}; see Figure 4a).

SCHEME 1

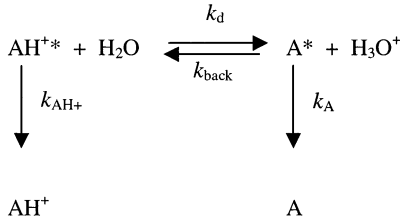

Assuming that the apparently complex reprotonation of A* can be represented by the unimolecular rate constant k_{back}, the data were analyzed in terms of eqs 2−6, readily derived from the simple prototropic kinetics depicted in Scheme 1.[8]

$$X = k_d + k_{AH^+} = \frac{R\lambda_3 + \lambda_2}{R + 1} \quad (2)$$

$$Y = k_{back} + k_A = \lambda_3 + \lambda_2 - X \quad (3)$$

$$k_d = X - k_{AH^+} \quad (4)$$

$$k_{back} = \frac{XY - \lambda_3\lambda_2}{k_d} \quad (5)$$

$$k_A = Y - k_{back} \quad (6)$$

The rate constant for excited state deprotonation, k_d (eq 4), is pH-independent, with the value of $k_d = (3.4 \pm 0.4) \times 10^{10}$ s^{-1}. This value is only ca. 5-fold smaller than in water in the absence of SDS micelles ($k_d = 1.5 \times 10^{11}$ s^{-1}), as opposed to the 40-fold reduction of k_d for deprotonation of AH^+ in the ground state (from 1.4×10^6 s^{-1} in water to 3.6×10^4 s^{-1} in SDS).[3,6] Clearly, then, the preferential stabilization of the positively charged flavylium ion AH^+ (relative to the neutral anhydrobase, A) by the anionic SDS micelle has a substantially smaller impact on the deprotonation rate constant in the excited state than in the ground state. This decrease in the effect of SDS on the rate constant is consistent with the greater acidity of the excited state, i.e., with a significant shift of electron density from the oxygen of the 7-OH group into the positively charged flavylium ring system upon excitation.[3]

As expected from Scheme 1 and shown in Figure 7, the rate constant k_{back} (eq 5) is a linear function of $[H^+]_w$, the concentration of protons in the intermicellar aqueous phase. However, as implied by the peculiar pH dependence of $R = A_3/A_2$ at pH > 3, the intercept of the plot in Figure 7 is not zero. Consequently, k_{back} must have the functional form: $k_{back} = k_r + k_p[H^+]_w$. Indeed, the value of the apparent reprotonation rate constant (referred to $[H^+]_w$) of excited A, $k_p = (1.57 \pm 0.15) \times 10^{11}$ L mol^{-1} s^{-1}, is only slightly smaller than that of ground state A ($k_p(S_0) = 1.8 \times 10^{11}$ L mol^{-1} s^{-1}) in SDS micelles. A similar slight decrease in k_p relative to $k_p(S_0)$ has been observed for several other flavylium salts in water and is compatible with the fact that A is a weaker base in the excited state (excited AH^+ is a stronger acid) than in the ground state. As pointed out in previous work on the ground state reprotonation of anthocyanins in micellar SDS,[7] the pH-dependent bimolecular component (k_p) of the reprotonation of A* does not involve protonation by a micelle-bound proton but rather occurs via entry of a proton into the micelle from the aqueous phase, followed by encounter with the excited base on the micelle surface.

The fact that the intercept in Figure 7 is different from zero means that there is a second mechanism for reprotonation of

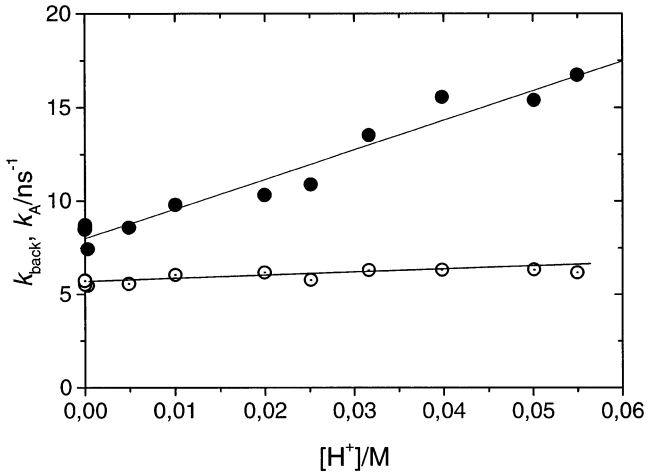

Figure 7. Plot of the k_{back} (●) and k_A (○) values obtained assuming simple acid−base kinetics (Scheme 1), as a function of $[H^+]$.

SCHEME 2

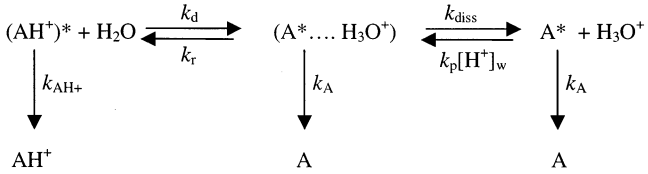

A*, with a rate constant of $k_r = (8.0 \pm 0.4) \times 10^9$ s^{-1}, that is independent of the intermicellar aqueous pH. Because it is independent of $[H]_w$, it must also be independent of $[H]_{mic}$, the local concentration of protons at the SDS micellar surface, which is controlled by proton/sodium counterion exchange at the micelle surface. Water can be ruled out as the proton donor because A* is a weaker base than the ground state A and the latter is not protonated by water in SDS micelles.[6,7] Participation of the buffer anions can be ruled out as well because the observed fluorescence decay is identical in the presence and absence of buffer at the same pH. Thus, the only remaining possibility is that the pH-independent component of the back protonation of A* involves a compartmentalized reaction, on the surface of the micelle, between A* and the proton that was generated by deprotonation of (AH^+)*.

The simplest scheme that is consistent with this possibility and with directly measured or estimated values of the rate constants is depicted in Scheme 2.

In this scheme, the initially formed compartmentalized pair at the micelle surface is depicted as $(A^*\cdots H_3O^+)$. The compartmentalized reprotonation reaction, characterized by the rate constant k_r, must compete with proton escape (k_{diss}) and the decay of A* to the ground state (k_A). The mechanism of Scheme 2 translates into the differential eq 7:

$$\frac{d}{dt}\begin{bmatrix} AH^+ \\ A\cdots H^+ \\ A \end{bmatrix} = \begin{bmatrix} -X & k_r & 0 \\ k_d & -Y & k_p[H^+]_w \\ 0 & k_{diss} & -Z \end{bmatrix} \times \begin{bmatrix} AH^+ \\ A\cdots H^+ \\ A \end{bmatrix} \quad (7)$$

where X, Y, and Z are given by eqs 8−10.

$$X = k_d + k_{AH^+} \quad (8)$$

$$Y = k_r + k_{diss} + k_A \quad (9)$$

$$Z = k_p[H^+]_w + k_A \quad (10)$$

Equation 7 predicts triple exponential time-dependent functions for the three species (AH^+, compartmentalized pair, and

A), where the three reciprocal decay times (λ_i) are the roots of the third order eq 11.

$$\begin{bmatrix} \lambda - X & k_r & 0 \\ k_d & \lambda - Y & k_p[H^+]_w \\ 0 & k_{diss} & \lambda - Z \end{bmatrix} = 0 \qquad (11)$$

The above formalism is considerably simplified under conditions such that $k_p[H^+]_w$ can be neglected with respect to k_A, i.e., when proton escape is irreversible. Taking $k_p = 1.6 \times 10^{11}$ L mol^{-1} s^{-1} and the reciprocal lifetime of A* ($k_A = 5 \times 10^9$ s^{-1}), such conditions are verified within 3% error for pH values higher than 3.

The three solutions of eq 11 (denominated λ_2, λ_3, and λ_4, retaining the designation λ_1 for the long-lived component in the emission of AH*) in the limit of $k_p[H^+]_w = 0$ are (eqs 12 and 13)

$$\lambda_{3,2} = \frac{X + Y \pm \sqrt{(X - Y)^2 + 4k_r k_d}}{2} \qquad (12)$$

$$\lambda_4 = k_A \qquad (13)$$

The derivation of relations between the rate constants and decay parameters (λ_i) and the preexponential ratio ($R = A_3/A_2$) is also straightforward.

$$X = \frac{R\lambda_3 + \lambda_2}{R + 1} \qquad (14)$$

$$Y = \lambda_3 + \lambda_2 - X \qquad (15)$$

$$k_d = X - k_{AH^+} \approx X \qquad (16)$$

$$k_r = \frac{XY - \lambda_3\lambda_2}{k_d} \qquad (17)$$

$$k_{diss} = Y - k_A - k_r \qquad (18)$$

In addition to the kinetically uncoupled, long-lived fraction of $(AH^+)^*$, which is not shown explicitly, Scheme 2 implies the presence of three kinetically coupled species, deprotonable $(AH^+)^*$, the compartmentalized pair $(A^*\cdots H_3O^+)$, and A*. In general, this should lead to tetraexponential decays at the emission wavelength of $(AH^+)^*$ and triexponential decays at the emission wavelength of A*. In the particular case of pH > 3 (no back reaction of the last species, A*), triexponential decays are predicted at both of the emission wavelengths, but only two of the three decay times should be common for both emissions: $\tau_3 = 1/\lambda_3$ and $\tau_2 = 1/\lambda_2$. At the emission wavelength of $(AH^+)^*$, the third decay time (τ_1) should be assigned to the kinetically uncoupled $(AH^+)^*$, while at the emission wavelength of A*, the third lifetime should be equal to the lifetime of A* ($1/k_A$).

Experimentally, we observe triexponential rather than tetraexponential decay of $(AH^+)^*$. Because the longest lifetime (τ_1) corresponds, as noted above, to the uncoupled species, the two shorter lifetimes, τ_3 and τ_2, are assigned to the kinetically coupled species $(AH^+)^*$ and $(A^*\cdots H_3O^+)$. Likewise, at the emission wavelength of A*, we observe biexponential rather than triexponential decay, implying that two of the three predicted lifetimes are experimentally (mathematically) indistinguishable. Indeed, as indicated by the data of Figure 4a, the intermediate decay time (τ_2) is essentially equal to the independently measured lifetime of the excited base ($1/k_A$).

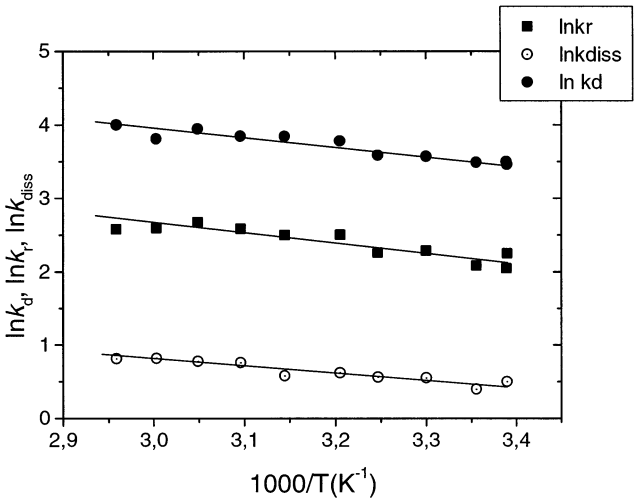

Figure 8. Arrhenius plots of the rate constants of deprotonation, k_d (●), dissociation of the compartmentalized pair, k_{diss} (○), and recombination of the compartmentalized pair, k_r (■) evaluated from eqs 16−18.

TABLE 2: Values of the Rate Constants at 22 °C (k^{295}), Apparent Activation Energies (E), and Preexponential Factors (k^0) of the Kinetic Processes of HMF in the First Excited Singlet State in 0.10 M Micellar Solutions of SDS

	k^{295} (ns^{-1})	E (kJ mol^{-1})	k^0 (ns^{-1})
decay of $(AH^+)^*$ (k_{AH^+})	0.18		
deprotonation of $(AH^+)^*$ (k_d)	34	10.1 ± 1.2	2000
recombination of $(A^*\cdots H^+)$ (k_r)	8.8	9.8 ± 1.7	486
dissociation of $(A^*\cdots H^+)$ (k_{diss})	1.6	7.6 ± 1.0	35
protonation of A* ($k_p[H^+]$; $[H^+] = 1$ M)	157		
decay of A* (k_A)	5.0		
rotation of the uncoupled $(AH^+)^*$ (k_{rot})	1.2	22.1 ± 0.2	97000

Reanalysis of the experimental decay parameters (λ_3, λ_2, R, and k_A) in terms of Scheme 2 (via eqs 14−18) provides the results shown in Figure 8 and Table 2. The values of the rate constants for deprotonation of $(AH^+)^*$ and of recombination of the compartmentalized pair to yield back the excited acid, $(AH^+)^*$, are the same as those encountered employing Scheme 1 (at 22 °C, $k_d = 3.4 \times 10^{10}$ s^{-1} and $k_r = 8.8 \times 10^9$ s^{-1}, respectively). The value of the dissociation rate constant of the compartmentalized pair ($k_{diss} = 1.6 \times 10^9$ s^{-1} at 22 °C) is 5-fold lower than k_r, which validates our assumption that the recombination of the compartmentalized pair can compete with its dissociation, although only ca. 15% of the compartmentalized pairs undergo net deprotonation to A*.

The apparent activation energies for formation and back recombination of the compartmentalized pair are equal within experimental error ($E_d = 10.1 \pm 1.2$ kJ mol^{-1} and $E_r = 9.8 \pm 1.7$ kJ mol^{-1}, respectively).[12] Low activation energies are consistent with the high acidity of the excited singlet state of AH^+.[13] The apparent activation energy for dissociation of the geminate pair ($E_{diss} = 7.7 \pm 1.0$ kJ mol^{-1}) is also small, consistent with lateral diffusive migration of the proton on the SDS micellar surface but not with proton exit from an anionic micelle.

Conclusions

The deprotonation of excited HMF is sufficiently fast to enable discrimination between two subpopulations of HMF in the SDS micelle, one of which consists of molecules that are

in orientations appropriate for prompt proton transfer at the moment of excitation, i.e., with the OH group in contact with water at the micelle surface and the other of molecules in orientations that must rotate to expose the OH group to water. The rotational reorientation times range from ca. 800 ps at 22 °C to 270 ps at 65 °C ($k_{rot} = 1.2 \times 10^9$ s^{-1} at 22 °C and $E_{rot} =$ 22 kJ mol^{-1}), suggesting that HMF may be a useful probe for rotational mobility in micelles.

On the micelle surface, the kinetics of the overall excited state proton transfer process require a minimum of three species, the excited acid $(AH^+)^*$, the micelle-compartmentalized pair $(A^*\cdots H_3O^+)$, and the excited base A*. Of particular interest is the nature of this compartmentalized pair, which can be inferred from a consideration of the magnitudes of the rate constants involved. Both the rate of decay of A* ($k_A = 5 \times 10^9$ s^{-1}) and the rate constant for dissociation of the compartmentalized pair ($k_{diss} = 1.6 \times 10^9$ s^{-1} at 22 °C) are roughly an order of magnitude larger than the exit rate constant of a proton from an SDS micelle under our experimental conditions (which we estimate to be ca. $1-2 \times 10^8$ s^{-1}).[14] Consequently, the entire excited state proton transfer process occurs so rapidly and the lifetimes of the excited species involved in this process are so short that only a very minor fraction (<1−2%) of the protons generated by deprotonation of $(AH^+)^*$ would have time to exit from the micelle prior to decay of A* back to the ground state! Thus, in Scheme 2, the species $(A^*\cdots H_3O^+)$ must be a geminate compartmentalized pair. Deprotonation of $(AH^+)^*$ initially forms the geminate pair (k_d), which in turn can recombine (k_r) to restore $(AH^+)^*$. Alternatively, dissociation of this pair on the micelle surface (k_{diss}) leads to A*, which is formally still a micelle-compartmentalized pair but no longer geminate. The present study thus provides a rather detailed kinetic picture of the initial steps involved in an ultrafast excited state proton transfer process at the surface of a typical anionic micelle.

Acknowledgment. This work was partially supported by the research grants PRAXIS/PCEX/C/QUI/56/96, ICCTI/CAPES/423, and POCTI/QUI/33679/99. A.L.M. acknowledges the Program CIENCIA (FCT, Portugal) for partial funding in the acquisition of the picosecond laser system. J.C.L. is grateful to FCT-Fundação para a Ciência e Tecnologia for a postdoctoral grant (PRAXIS 4/4.1/BPD/3410). C.Y. acknowledges a doctoral fellowship from the Fundação de Amparo à Pesquisa do Estado de São Paulo (FAPESP). F.H.Q. thanks FAPESP for additional funding and the Conselho Nacional de Desenvolvimento Científico e Tecnológico (CNPq), Brasília for a senior research fellowship.

References and Notes

(1) Arnaud, L. G.; Formosinho, S. J. *J. Photochem. Photobiol. A: Chem.* **1993**, *75*, 1−20.

(2) Tolbert, L. M.; Solnetsev, K. M. *Acc. Chem. Res.* **2002**, *35*, 19−27.

(3) Maçanita, A. L.; Moreira, P.; Lima, J. C.; Quina, F.; Yihwa, C.; Vautier-Giongo, C. *J. Phys. Chem. A* **2002**, *106*, 1248−1255.

(4) Bunton, C. A.; Nome, F. J.; Quina, F. H.; Romsted, L. S. *Acc. Chem. Res.* **1991**, *24*, 357.

(5) Pramauro, E.; Pelizzetti, E. *Surfactants in Analytical Chemistry -Applications of Organized Amphiphilic Media*; Elsevier: Amsterdam, 1996.

(6) Vautier-Giongo, C.; Yihwa, C.; Moreira, P. F., Jr.; Lima, J. C.; Freitas, A. A.; Alves, M.; Quina, F. H.; Maçanita, A. L. *Langmuir*, in press.

(7) Lima, J. C.; Vautier-Giongo, C.; Lopes, A.; Melo, E. C.; Quina, F. H.; Maçanita, A. L. *J. Phys. Chem. A* **2002**, *106*, 5851−5859.

(8) Lima, J. C.; Abreu, I.; Brouillard, R.; Maçanita, A. L. *Chem. Phys. Lett.* **1998**, *298*, 189.

(9) Striker, G.; Subramaniam, V.; Seidel, C. A. M.; Volkmer, A. *J. Phys. Chem. B* **1999**, *103*, 8612−8617.

(10) Chou, S. H.; Wirth, M. J. *J. Phys. Chem.* **1989**, *93*, 7694−7698. (b) Wirth, M. J.; Chou, S. H.; Piasecki, D. A. *Anal. Chem.* **1991**, *63*, 146−151. (c) Maiti, N. C.; Krishna, M. M. G.; Britto, P. J.; Periasamy, N. *J. Phys. Chem.* **1997**, *101*, 11051−11060. (d) Carroll, M. K.; Unger, M. A.; Leach, A. M.; Morris, M. J.; Ingersoll, C. M.; Bright, F. V. *Appl. Spectrosc.* **1999**, *53*, 780−784.

(11) Zachariasse, K. A. *Chem. Phys. Lett.* **1978**, *57*, 429. (b) Maçanita, A. L. Ph.D. Thesis, I. S. T.−University Técnica de Lisboa, 1981.

(12) The fact that deprotonation of $(AH^+)^*$ is faster than recombination of $(A^*\cdots H^+)$ is due exclusively to the higher preexponential factor of the former ($k_d^0 = 2 \times 10^{12}$ s^{-1} vs $k_r^0 = 4.9 \times 10^{11}$ s^{-1}). This in turn suggests that the change in entropy associated with the formation of the geminate pair is slightly positive rather than strongly negative as should be observed if the proton in the geminate pair was fully hydrated.[13] The finding that the preexponential factor for dissociation of the geminate pair ($k_{diss}^0 = 3.5 \times 10^{10}$ s^{-1}) is smaller than that for recombination is in line with an increase in the degree of hydration of the proton during separation of the geminate pair.

(13) Robinson, G. W.; Thistlethwaite, P. J. *J. Phys. Chem.* **1986**, *90*, 4224−4233.

(14) As noted previously,[7] under our conditions, the ratio of the local concentrations of micelle-bound to aqueous protons is roughly 80, which for a surfactant molar volume of 0.25 M^{-1} and an aggregation number of ca. 75, corresponds to a ratio of micellar entry and exit rate constants of the proton from the SDS micelle of $k_{+H}/k_{-H} \approx 1500$. Thus, assuming that the overall pH-dependent reprotonation process is close to diffusion-controlled, i.e., that $k_{+H} \approx 1-2 \times k_p$, one obtains an estimate of $k_{-H} \approx (1-2) \times 10^8$ s^{-1} under our conditions (0.10 M SDS, added sodium phosphate buffer present).